Turbulent Pipe Flow at Extreme Reynolds Numbers

M. Hultmark, M. Vallikivi, S. C. C. Bailey, and A. J. Smits

Turbulent Pipe Flow at Extreme Reynolds Numbers

M. Hultmark,[1] M. Vallikivi,[1] S. C. C. Bailey,[2] A. J. Smits[1]

[1] *Department of Mechanical and Aerospace Engineering,*
Princeton University, Princeton, NJ, 08540, USA,

[2] *Department of Mechanical Engineering, University of Kentucky, Lexington, KY 40506, USA*

Both the inherent intractability and complex beauty of turbulence reside in its large range of physical and temporal scales. This range of scales is captured by the Reynolds number, which in nature and in many engineering applications can be as large as 10^5-10^6. Here, we report turbulence measurements over an unprecedented range of Reynolds numbers using a unique combination of a high-pressure air facility and a new nano-scale anemometry probe. The results reveal previously unknown universal scaling behavior for the turbulent velocity fluctuations, which is remarkably similar to the well known scaling behavior of the mean velocity distribution.

Most practical flows are turbulent. For example, the flow in a river, over a large vehicle, or in the lower atmosphere, is almost always turbulent, and the turbulent velocity field is often described as consisting of a large number of eddying motions, an observation first recorded by Leonardo da Vinci [1]. The eddies cause intense mixing to take place, and therefore turbulent flows are very effective in transporting momentum, energy, and mass. What makes turbulence so challenging, and our predictions so fickle, is that the eddies cover a very large range of sizes. One measure of the flow complexity is given by the magnitude of the Reynolds number Re^+, which is the ratio of the size of the largest eddies, set by the size of the flow domain R (e.g. radius in pipe flow), to the size of the smallest eddies η, set by the viscous dissipation of energy, so that $Re^+ = R/\eta$. In high Reynolds number turbulent flows, which include many flows of great practical interest, such as the atmospheric surface layer or the flow in large pipes, $Re^+ = \mathcal{O}(10^5$-$10^6)$. Under these conditions, direct computations of turbulence are extremely challenging, and experiments become essential to develop turbulence models and scaling rules to help predict the behavior of turbulent flows.

We are particularly interested in the behavior of high Reynolds number flows, where there is a large separation of scales between the largest and smallest eddies. In fact, almost all theories of turbulence are only valid in the high Reynolds number limit. Field experiments are notoriously difficult, however, and to achieve large Reynolds numbers in the laboratory we need to make either R large, or η small, or do both, which is usually difficult and expensive. McKeon *et al.* [2] and Morrison *et al.* [3] used the Princeton Superpipe, in which pipe flow turbulence can be studied at very high Reynolds numbers by using compressed air at pressures, p_a, up to 220 atm as the working fluid [4]. High pressure brings the realm of high Reynolds number into a modest scale laboratory, and it is relatively inexpensive to produce a very high quality flow. Our current experimental setup is shown in figure 1a and figure 1b. However, at the highest

Reynolds number possible in the Superpipe apparatus, η can be as small as 0.3 μm [5], and to measure all aspects of the turbulence we need to have instrumentation capable of resolving these small scales. Only then will we have the capability to learn exactly how turbulence varies with Reynolds number, which will provide the empirical basis for theory and computation of turbulent flows in nature and industry. The preferred instrument for turbulence studies has always been the hot-wire anemometer, because it gives a continuous time signal and is thus able to temporally resolve the turbulent motions. However, the sensor must be small enough to avoid the phenomenon of spatial filtering, where the energy contained in eddies smaller than the sensor length is effectively filtered from the signal.

It is difficult to make hot-wire sensors smaller in length than about 0.25 mm, which is generally much larger than η in high Reynolds number flow. Therefore, to resolve the smallest scales in the Superpipe, a new solution needed to be found. Our approach was to develop a Nano-Scale Thermal Anemometry Probe (NSTAP) [6, 7], a free-standing nanoscale Platinum wire with cross-section of 2 μm by 100 nm and active length, ℓ, as small as 30 μm, suspended between two electrically conducting supports. A sketch of a typical NSTAP, with 60 μm long wire, is shown in figure 1c and a scanning electron microscope image of a fabricated probe is shown in figure 1d.

We have now combined the Superpipe facility with the NSTAP to investigate the scaling behavior of turbulence at very high Reynolds numbers. In the traditional view, the mean flow scaling in, for example, pipe flow, can be divided into three distinct regions at asymptotically infinite Reynolds numbers. The first is the near-wall region, where the characteristic velocity scale is the friction velocity u_τ and the characteristic length scale is the viscous length scale, ν/u_τ. Here, $u_\tau = \sqrt{\tau_w/\rho}$, where τ_w is the wall shear stress, and ρ and ν are the density and kinematic viscosity of the fluid, respectively. Note that for pipe and boundary layer flows, a reasonable measure of η, the scale of the smallest eddies, is given by ν/u_τ, so
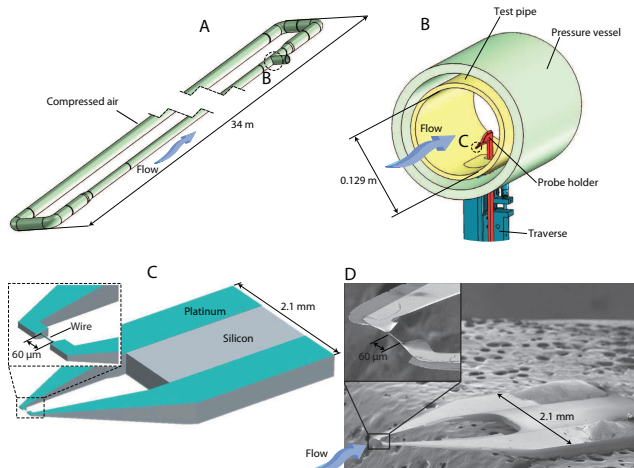
FIG. 1. Experimental setup and device. a) sketch of Super-pipe; b) Close-up of the test section with the pressure vessel, test pipe, and probe holder; c) Drawing of the NSTAP with 60 μm sensing element; d) SEM images of a typical 60μm NSTAP probe.

that $Re^+ = Ru_\tau/\nu$. The near-wall region is often described as extending from the wall out to approximately $y^+ = 50$. Here, y is the wall-normal distance, and all "plus" variables are non-dimensionalized using u_τ and ν/u_τ, so-called inner variables. Beyond $y/R \approx 0.12$ a wake region exists, where the mean velocity scales with outer variables, that is, it is a function of y/R and u_τ. One of the primary difficulties with wall-bounded turbulent flows is that it is a two-scale problem, in other words, the inner and outer region scale according to two different sets of variables. This observation, however, leads to a major result based on an overlap argument, where at a sufficiently high Reynolds number there would exist between the near-wall and the wake regions a region where the mean velocity follows a logarithmic law [8] given by

$$U^+ = \frac{1}{\kappa} \ln y^+ + B \qquad (1)$$

and κ and B are constants.

However, the very high Reynolds number mean velocity experiments by McKeon *et al.* [2], in the Princeton Superpipe, revealed that the mean velocity follows logarithmic scaling only in the region $600\nu/u_\tau \leq y \leq 0.12R$. Between approximately $y^+ = 50$ and 600, the mean velocity instead follows a power law, $U^+ = A(y^+)^n$, where A and n are Reynolds number independent constants. Therefore the log-law does not appear for Reynolds numbers less than about 5×10^3, and a decade of log-law does not appear until $Re^+ > 5 \times 10^4$, a value that is well beyond the reach of most laboratory facilities.

Although the mean velocity scaling behavior is now well established, finding the equivalent scaling behavior for the turbulence quantities has been particularly elu-
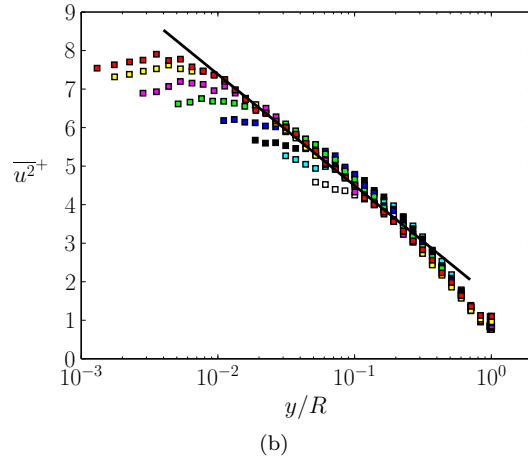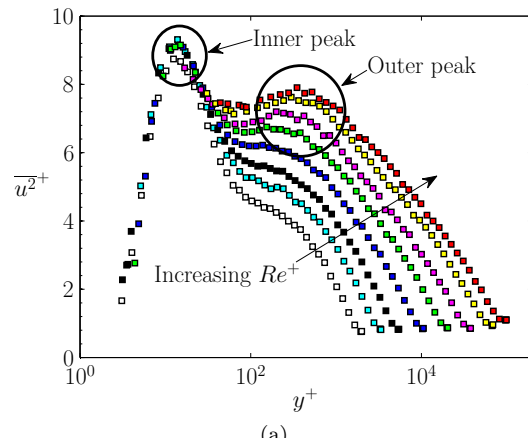

(a)

(b)

FIG. 2. Turbulence fluctuations for $Re^+ = 1985$, 3334, 5411, 10481, 20251, 37450, 68371 and 98187. (a) Inner scaled. Circles show inner and outer peak. (b) Outer scaled. Only $y^+ > 100$ shown for clarity. Solid line is the log-law of the turbulent fluctuations.

TABLE I. Experimental conditions

$Re_D = 2R\langle U \rangle/\nu$	Re^+	p_a [atm]	$\langle U \rangle$ [m/s]	ℓ [μm]	ℓ^+
81×10^3	1,985	1.0	9.5	60	1.8
146×10^3	3,334	1.7	10.1	60	3.1
247×10^3	5,411	3.2	8.4	60	5.0
513×10^3	10,481	6.4	9.4	60	9.7
1.1×10^6	20,251	11.5	10.8	60	18.8
2.1×10^6	37,450	23.4	10.5	30	17.4
4.0×10^6	68,371	46.9	10.4	30	31.7
6.0×10^6	98,187	70.7	10.6	30	45.5

sive. The Reynolds number scaling of the streamwise Reynolds stress, $\overline{u^2}^+$, which describes the intensity of the turbulence, has been the subject of particularly intensive research. Here, we report the scaling behavior of $\overline{u^2}^+$ over an unprecedented range of Re^+ and degree of accuracy (see table I for more details). Figure 2a shows

the resulting values of $\overline{u^2}^+$ (corrected for spatial filtering effects according to Smits et al. [9]) as a function of distance from the wall in inner coordinates, y^+, for all Reynolds numbers measured. We begin by examining the results in the near-wall region. Of particular interest in this region is the scaling behavior of the near-wall peak in $\overline{u^2}^+$ located at $y^+ \approx 15$. This peak is associated with the location where the turbulence production rates are highest. In the past, it had been postulated that the near-wall turbulence was driven solely by the presence of the wall and therefore $\overline{u^2}^+$ would depend on inner variables alone. Earlier studies appeared to support this hypothesis, but results from the high Reynolds number atmospheric surface layer and direct numerical simulations at low Reynolds numbers indicate that the magnitude of this peak is Reynolds number dependent due to interaction between near-wall eddies and those further from the wall [10]. In contrast, recent low Reynolds number results from the Superpipe, presented by Hultmark *et al.* [11], indicate that the near-wall peak is independent of Reynolds number, and collapses in inner variables.

The results shown in figure 2a clearly demonstrate that the magnitude of the near-wall peak in $\overline{u^2}^+$ at $y^+ \approx 15$ remains constant, at least up to the highest Reynolds number where it could be resolved. Our present results therefore conclusively support Hultmark *et al.*'s low Reynolds number observations, and confirm that the near-wall peak scales on inner variables alone, at least for pipe flows.

In addition to the inner peak at $y^+ \approx 15$, the results presented in figure 2a also reveal the presence of an outer peak between $100 < y^+ < 800$ for the three highest Reynolds numbers measured. Morrison *et al.* [3] reported similar behavior, but their observations are frequently dismissed since at their highest Reynolds numbers spatial filtering undoubtedly had a significant impact on their measurements. However, the current results demonstrate conclusively that the existence of this outer peak is a genuine feature of high Reynolds number turbulence, and not simply an artifact of spatial filtering. Furthermore, we can find the position of the outer peak as a function of Reynolds number as $y_p^+ = 0.23(Re^+)^{0.67}$.

The presence of an outer peak has several important implications for wall-bounded turbulence at extreme Reynolds numbers. First, none of the many turbulence models that are used in Reynolds-averaged Navier-Stokes methods will predict its appearance, representing a fundamental flaw in turbulence modeling. The primary reason is that the turbulence is coupled to the mean velocity gradient, and since the gradient decreases monotonically with distance from the wall, such models will never predict a non-monotonic turbulence behavior. Second, assuming that the magnitude of the inner peak continues to remain constant with Reynolds number, at some Reynolds number the magnitude of the outer peak will
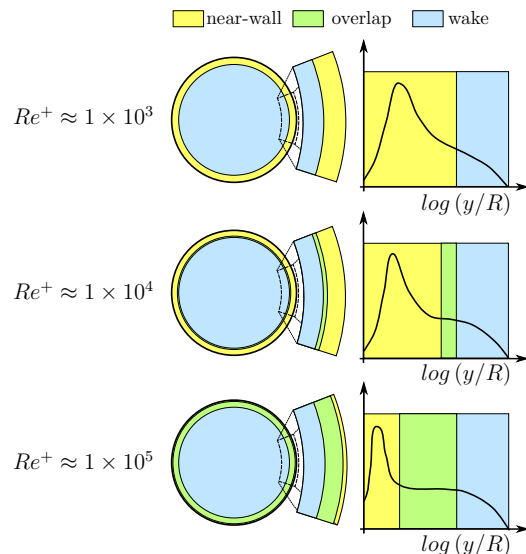

FIG. 3. Schematic of the different regions of the flow at different Reynolds numbers. To the left in physical space and to the right on a logarithmic axis. The graph shows the production of turbulence kinetic energy in premultiplied form (so that equal areas under the graph corresponds to equal contributions to the total production).

exceed that of the inner peak, since it will continue to increase with Reynolds number. Such behavior would reflect a shift in the turbulence production away from the wall with increasing Re^+ as a consequence of the continually increasing separation of scales. Although the rate of turbulence production will always be a maximum closest to the wall, our results imply that the peak production will increasingly occupy a smaller physical region in the flow as the Reynolds number increases. As illustrated in figure 3, although the production rates are lower further away from the wall, turbulence is produced over an increasingly larger area relative to that corresponding to the near wall production.

The location where the outer peak develops is above $y^+ > 50$, a region where the mean flow is traditionally expected to scale logarithmically (see for example, textbooks such as Pope [12]). Within this region, Townsend [13] hypothesized that turbulence production and dissipation should be in equilibrium. However, the development of the outer peak implies that such an equilibrium does not exist in the region of the outer peak ($y^+ \lesssim 800$) since the presence of the peak indicates production exceeds dissipation here. As a result, we should not expect true logarithmic scaling of the mean flow this close to the wall, consistent with the results of McKeon *et al.* [2], who found that logarithmic scaling in the mean flow did not emerge until $y^+ \gtrsim 600$.

We now shift our attention to this logarithmically scaled region, which forms as an overlap layer between inner and outer scaled regions of the mean flow. It has

been suggested by Townsend [13] and Perry *et al.* [14] that at a sufficiently high Reynolds numbers where the overlap layer forms, the turbulence intensity $\overline{u^2}^+$ should also follow a logarithmic variation such that

$$\overline{u^2}^+ = B_1 - A_1 \ln\left(\frac{y}{R}\right). \qquad (2)$$

The existence of such a region has never been fully validated due to the limited range of Reynolds numbers achieved in previous laboratory studies, although hints of a logarithmic turbulence behavior have been observed in data from the atmospheric surface layer [15]. By plotting the streamwise turbulent fluctuations against y/R, as in figure 2b, our results conclusively demonstrate the existence of such a logarithmic behavior for the turbulence intensity. A regression fit of the three highest Reynolds numbers indicates that $B_1 = 1.61$ and $A_1 = 1.25$. Perry *et al.* [14] argued that the constant A_1 is related to the hierarchy of large eddies in the flow and directly proportional to the eddy-intensity function as introduced by Townsend [13]. Perry *et al.* further argued that in pipe flow the large eddies are influenced by geometric effects with eddies from the opposing side penetrating into the flow. However, the existence of a log law in the current results indicate that only eddies in the wake region are affected by the geometry.

The measurements presented here are the first to show the logarithmic scaling of the fluctuations, and that it only becomes evident for $y/R < 0.12$ once $Re^+ \gtrsim 20 \times 10^3$, with an increasing spatial extent with Reynolds number. At the highest Reynolds number measured, it spans more than 10% of the pipe radius. The appearance of this extended logarithmic variation marks the onset of the extreme Reynolds number range for pipe flow. The observation that very high Reynolds number turbulence displays some distinguishing characteristics has been noted in other flows as well [see, for example, 16].

One particularly interesting observation which we can make from figure 2b is that the Reynolds number at which the logarithmically-scaled $\overline{u^2}^+$ region appears is approximately the same as the one where the outer peak emerges. Because the logarithmic region extends all the way to the outer peak, we can infer that the outer peak forms as a result of increased scale separation between the inner-scaled turbulent motions produced at the wall and the outer-scaled turbulent motions produced further from the wall.

When comparing profiles of the fluctuating and mean velocities for very high Reynolds numbers, as is done in figure 4, we find that the same regions identified by McKeon *et al.* [2] for the mean velocity profile are also observed in the turbulence profile. The region where the inner peak in $\overline{u^2}^+$ exists corresponds to the near-wall region, where the mean velocity and turbulence profiles scale on inner variables. The region between the inner and outer peaks is a blending region where the mean
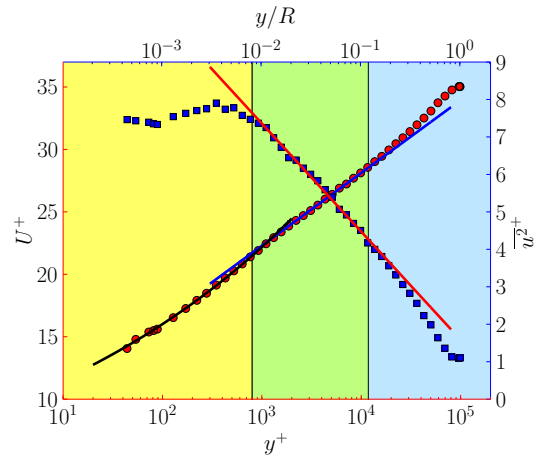

FIG. 4. Comparison of mean velocity and turbulence streamwise fluctuation profiles for $Re^+ = 98 \times 10^5$. Red symbols are mean velocities, blue solid line the log-law for the mean velocity and the black solid line is the power-law for the mean velocities as described by McKeon *et al.* [2]. Blue symbols are the turbulence fluctuations and the red solid line is the log-law for the fluctuations, as reported in this letter.

profile exhibits a power law behavior ($50 \lesssim y^+ \lesssim 800$). Further away from the wall, both the mean and turbulence intensity follow a logarithmic behavior extending up to $y/R = 0.12$. Finally, an outer region can be identified for $y/R > 0.12$ where the mean velocity and the turbulence intensity scale using outer variables.

These four regions are only truly distinct at the extremely high Reynolds numbers measured in the current study. For lower Reynolds numbers, no separation exists between $y^+ < 800$ and $y/R > 0.12$ and therefore the logarithmic region is not evident, neither in the mean velocity nor in the turbulence. This high degree of correspondence was previously unknown, and presents an important simplification in the modeling of wall-bounded turbulence.

In particular, at these extremely high Reynolds numbers the logarithmically scaled overlap layer will increasingly dominate the near wall flow, occupying as much as 12% of the pipe radius, whereas the inner-scaled region at these Re^+ values will occupy much less than 1%. Correspondingly, a greater percentage of turbulence production will also move to the overlap layer and, at extremely high Reynolds numbers, the near-wall turbulence production cycle will ultimately become irrelevant.

[1] Note1, see, for example, "Deluge", a drawing by Leonardo da Vinci dating from 1511-1515, held in the Royal Library, Windsor Castle.

[2] B. J. McKeon, J. Li, W. Jiang, J. F. Morrison, and A. J. Smits, J. Fluid Mech. **501**, 135 (2004).

[3] J. F. Morrison, B. J. McKeon, W. Jiang, and A. J. Smits, J. Fluid Mech. **508**, 99 (2004).

[4] M. V. Zagarola and A. J. Smits, J. Fluid Mech. **373**, 33 (1998).

[5] V. Yakhot, S. C. C. Bailey, and A. J. Smits, J. Fluid Mech. **652**, 65 (2010).

[6] S. C. C. Bailey, G. J. Kunkel, M. Hultmark, M. Vallikivi, J. P. Hill, K. A. Meyer, C. Tsay, C. B. Arnold, and A. J. Smits, J. Fluid Mech. **663**, 160 (2010).

[7] M. Vallikivi, M. Hultmark, S. C. C. Bailey, and A. J. Smits, Experiments in Fluids pp. 1–7 (2011).

[8] H. Tennekes and J. L. Lumley, *A First Course in Turbulence* (The MIT Press, Cambridge, Massachusetts, 1972).

[9] A. J. Smits, J. Monty, M. Hultmark, S. C. C. Bailey, M. Hutchins, and I. Marusic, J. Fluid Mech. **676**, 41 (2011).

[10] A. J. Smits, B. J. McKeon, and I. Marusic, Annu. Rev. Fluid Mech. **43**, 353 (2011).

[11] M. Hultmark, S. C. C. Bailey, and A. J. Smits, J. Fluid Mech. **649**, 103 (2010).

[12] S. B. Pope, *Turbulent Flows* (CUP, 2000).

[13] A. A. Townsend, *The Structure of Turbulent Shear Flow* (CUP, Cambridge, UK, 1976).

[14] A. E. Perry, S. M. Henbest, and M. S. Chong, J. Fluid Mech. **165**, 163 (1986).

[15] M. Metzger, B. J. McKeon, and H. Holmes, Phil. Trans. R. Soc. Lond. A **365**, 859 (2007).

[16] B. J. McKeon and J. F. Morrison, Phil. Trans. R. Soc. Lond. A **365**, 771 (2007).